CHAPTER 5

Hollow microneedles

CHAPTER 5

NOVEL HOLLOW MICRONEEDLE TECHNOLOGY FOR DEPTH CONTROLLED MICROINJECTION-MEDIATED DERMAL VACCINATION: A STUDY WITH POLIO VACCINE IN RATS

Koen van der Maaden[1*]
Bas Trietsch[2*]
Heleen Kraan[3]
Eleni Maria Varypataki[1]
Stefan Romeijn[1]
Raphäel Zwier[4]
Heiko van der Linden[2]
Gideon Kersten[1,3]
Thomas Hankemeier[2]
Wim Jiskoot[1]
Joke Bouwstra[1]

Pharmaceutical Research, 31 (2014) 1846–1854

[1] Division of Drug Delivery Technology, Leiden Academic Centre for Drug Research (LACDR), Leiden University
[2] Division of Analytical Biosciences, Leiden Academic Centre for Drug Research (LACDR), Leiden University
[3] Institute for Translational Vaccinology (Intravacc)
[4] Fine Mechanical Department, Leiden Institute of Physics (LION), Leiden University

[*] Authors contributed equally

Abstract

Purpose The aim of the study was to develop a cheap and fast method to produce hollow microneedles and an applicator for injecting vaccines into the skin at a pre-defined depth and test the applicability of the system for dermal polio vaccination.

Methods Hollow microneedles were produced by hydrofluoric acid etching of fused silica capillaries. An electromagnetic applicator was developed to control the insertion speed (1-3 m/s), depth (0-1000 µm), and angle (10°-90°). Hollow microneedles with an inner diameter of 20 µm were evaluated in *ex vivo* human skin and subsequently used to immunize rats with an inactivated poliovirus vaccine (IPV) by an intradermal microinjection of 9 µL at a depth of 300 µm and an insertion speed of 1 m/s. Rat sera were tested for IPV-specific IgG and virus-neutralizing antibodies.

Results Microneedles produced from fused silica capillaries were successfully inserted into the skin to a chosen depth, without clogging or breakage of the needles. Intradermal microinjection of IPV induced immune responses comparable to those elicited by conventional intramuscular immunization.

Conclusions We successfully developed a hollow microneedle technology for dermal vaccination that enables fundamental research on factors, such as volume, insertion depth, and insertion angle, on the immune response.

1. Introduction

Conventional vaccinations are performed by intramuscular or subcutaneous injections, causing pain and stress especially in toddlers and children. In addition, needlestick injuries and re-use of needles in developing countries carry the risk of transmitting biohazardous pathogens like hepatitis B and HIV. Because of the natural function of the skin, it is a highly immunologically active site. Therefore, it is not surprising that intradermal injections result in potent immune responses, but they are relatively difficult to perform and very painful [1]. Advances in microfabrication techniques are making intradermal injections using microneedles a feasible alternative to traditional injections. Microneedles can be used to only penetrate a shallow part of the skin (i.e. < 300 μm), thereby offering the possibility to deliver a vaccine into the epidermis or dermis, which is expected to yield a potent immune response. The minimally-invasive, potentially pain free nature and ease of the injections can reduce the risk of infections and alleviate the need for trained personnel [2-4].

One of the vaccines for which microneedle-based delivery would be advantageous is inactivated polio vaccine (IPV), as outlined below. Poliomyelitis, or polio, is a crippling and life-threatening disease that has been very effectively combated by widespread vaccination [5]. The majority of the vaccinations that helped to largely eradicate this disease have been performed using the oral polio vaccine (OPV) [6]. While very effective and easy to administer, this live attenuated vaccine can in rare cases revert to a pathogenic form and cause vaccine-associated paralytic poliomyelitis [7]. With reduced incidence of wild poliomyelitis and the associated change in risk/benefit considerations, the use of IPV has become the vaccination method of choice [8, 9]. While being a safer vaccine, IPV cannot be administered orally but is usually delivered using intramuscular or subcutaneous injection. Because of the widespread use of injected polio vaccines, switching to microneedles for less-invasive injections could benefit a large population by reducing infection risk and pain. Additionally, alleviating the need for trained personnel and dose sparing injections could reduce the costs of large vaccination programs [10, 11].

Among the available microneedles, hollow microneedles are especially attractive because the dose and the rate of drug delivery is controlled and there is no or limited need to reformulate the vaccine [2]. Hollow microneedles are commonly produced by pulling heated glass capillaries, using micromachining, or using microfabrication technologies on silicon wafers [12-15]. Pulled capillaries, however, may suffer from a low reproducibility in tip shape, low throughput production process and clogging problems because of a narrowing inner diameter towards the tip. While silicon needles can alleviate many of these problems, their production is complex and prohibitively expensive for routine use.

In this paper we present a novel microneedle fabrication method based on wet etching of capillaries that is cheap and easy to scale up. Batchwise fabrication of 100 microneedles can be performed in a lab without specialized equipment and the process can easily be adapted to the production of larger batches or even to a continuous process. The microneedles have a constant inner diameter, preventing clogging, and a tip shape that can be tuned with the

etch time. To ensure controlled and reproducible injection, we present a novel microneedle applicator. The penetration depth can be adjusted as well as the angle of insertion, the injection speed and time. We demonstrate reproducible injections in human skin *in vitro* and successful intradermal vaccination of rats with IPV using these hollow microneedles in combination with the applicator. This minimally-invasive, potentially pain free vaccination method resulted in a similar immune response as conventional intramuscular vaccination, showing the potential of etched microneedles for intradermal vaccination.

2. Materials and methods

2.1 Production of microneedles

Polyimide coated fused silica capillaries (Polymicro, Phoenix AZ, USA, 375 µm outer diameter, 20 µm inner diameter) were wet etched into microneedles. First, the lumen of the capillaries was filled with silicone oil AK350 (Boom Chemicals, Meppel, the Netherlands) to protect the inside of the capillary from the etchant. Subsequently, to etch the capillaries into microneedles, batches of up to 81 capillaries were mounted in a holder with one end suspended in 49% (w/w) HF, as shown in figure 1. The length of the capillary that is immersed in HF could be adjusted by the level of HF in the container as well as by the position of the screws of the holder during mounting. The shape of the microneedle tip was investigated as a function of etching time up to 30 hours. The microneedles chosen for the intradermal injections were etched for 4 hours. In order to connect the microneedles to the applicator, the sharp capillaries were glued into Luer adapters using medical grade glue (Loctite M-31 CL, Henkel, Düsseldorf, Germany). Luer adapters were acquired by removing the needle from Microlance® 26G hypodermic needles (BD, Franklin Lakes, NJ, USA). Finally, the polyimide coating was removed from the microneedles by submersion of the etched capillaries into hot sulfuric acid (96-98%, Boom chemicals, Meppel, the Netherlands) for 5 min at 200°C, and the silicone oil was removed by flushing the microneedles with acetone.

To assess the reproducibility of the tip shape, the tip angle of 55 microneedles with 20 µm inner diameter was measured after 4 hours etching. Image analysis was performed using ImageJ (available from rsbweb.nih.gov/ij/).

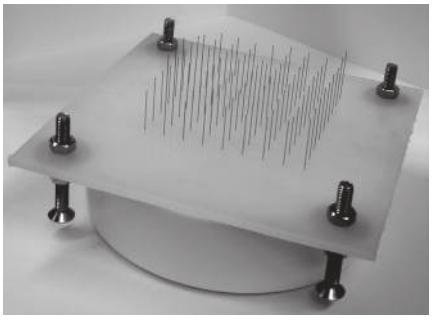

Figure 1: A batch of 81 fused silica capillaries mounted in a polyethylene holder and placed over a Teflon container with 49% HF. All needles are etched simultaneously by immersion in 49% HF. Immersion depth can be adjusted by the HF level in the container and the screw positions of the holder during mounting.

2.2 Microneedle applicator

In order to enable insertion of the microneedles into the skin to a controlled depth in a reproducible way, an applicator for hollow microneedles was developed. The flexibility of the skin can hamper skin penetration and reduce the depth accuracy of injections. The insertion speed, insertion depth, and angle of insertion are important factors to overcome this and achieve successful depth controlled penetration and drug delivery. As shown in figure 2, the applicator uses an electromagnet (a) to insert the microneedle mounted on the Luer connection (c) into the skin. The electromagnet is actuated using a controllable power source. Application of a variable current through the electromagnet allows for a tuned insertion speed from 1-3 m/s [16]. Furthermore, the controlled power supply regulates the wear time, to accurately and reproducibly control the time the microneedle is kept inside the skin. For injection, the skin is placed on a platform positioned below the injector (g). The penetration depth is controlled by a guide-plate (d) that can be adjusted with a micrometer actuator (b). The position of the guide-plate is adjusted so that the microneedle protrudes the desired distance through the hole in the plateau when the electromagnet is actuated. Before injection the injector is lowered so the guide-plate rests on top of the skin. Upon actuation the needle is inserted into the skin at the desired speed and depth, as controlled by the current and plateau position. Additionally the entire applicator can be tilted along a graduated rail (e) for angled insertion (10°-90° relative to the skin). Insertion at a shallow angle can be used to insert a greater length of the needle into the skin, without penetration into deeper skin layers. The hollow microneedles were attached to a syringe pump that was equipped with a gas tight Luer lock 100 µL syringe and connected to a fused silica capillary with a diameter of 100 µm (f) to allow tuning of the liquid delivery rate.

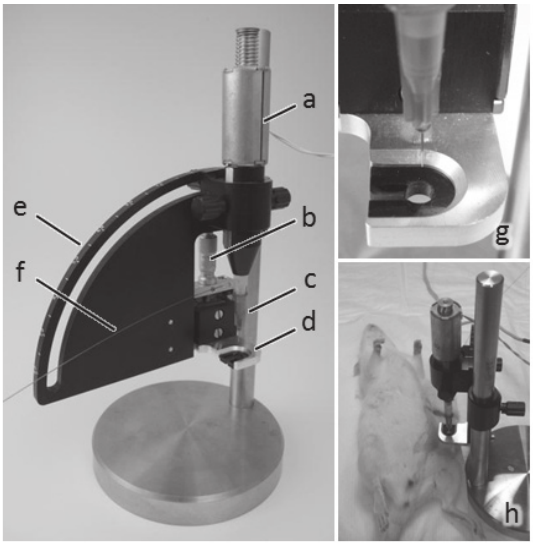

Figure 2: A microneedle applicator was developed using an electromagnet (a) to insert a microneedle (c) into the skin at controlled speed. A micrometer actuator (b) is used to adjust the level of a guide-plate (d) to ensure proper positioning and penetration depth of the microneedle. A graduated rail (e) can be used to tilt the entire applicator for angled insertion. The microneedle is connected to a syringe pump with a capillary (f) for vaccine delivery. Close-up of the guide-plate with a through hole for the needle (g). Microneedle applicator injecting a vaccine into the skin of an anesthetized rat (h).

2.3 Determination of microneedle insertion depth

To determine the microneedle insertion depth, fluorescently labeled human skin was used. *Ex vivo* abdominal or mammary human skin, which was obtained within 24 h after cosmetic surgery, was dermatomed to a thickness of 1200 µm using a Padgett Electro Dermatome Model B (Kansas City, MO, USA) after the fat was removed. The dermatomed skin was incubated overnight on filter paper soaked with 10 µg/mL fluorescein (Fluka®, Sigma-Aldrich, Steinheim, Germany) with the stratum corneum side to the surface in a Petri dish at 4°C. Before the skin was used for experiments, it was stretched on a piece of expanded polystyrene covered with parafilm, and thereafter the surface of the skin was cleaned 3 times with phosphate buffered saline (PBS) (Braun, Melsungen, Germany, pH 7.4, 163.9 mM Na^+, 140.3 mM Cl^-, 8.7 mM HPO_4^{2-}, and $H_2PO_4^-$). Subsequently, a microneedle was connected to the Luer connection on the microneedle applicator (figure 2c) and the micrometer actuator (figure 2d) was adjusted to a chosen depth up to 400 µm. In order to accurately set the insertion depth, the microneedle position was calibrated. First, the electromagnet was actuated and the microneedle was positioned to be flush with the plateau using the micrometer actuator (figure 2a). This was done by laser alignment, by which a laser was put perpendicular to the guide-plate of the applicator (figure 2d). When a microneedle protrudes past the guide-plate the laser light is scattered at the tip of the microneedle, therefore the needle was determined to be flush with the guide-plate at the point where no light scattering was observed at the microneedle tip. After this calibration of the microneedle position, the microneedle actuator was adjusted to a depth of 100, 200, 300, or 400 µm, and was subsequently pierced into the fluorescently labeled human skin. For each chosen depth 3 microneedles were used to pierce the skin and each microneedle stayed in the skin for 5 s. After the microneedles had pierced the fluorescently labeled skin, the microneedles were analyzed by bright-field microscopy and by fluorescence microscopy (Nikon Eclipse E600, mercury light source, GFP filter set) at 100x magnification and imaged with a 1 s exposure time. Subsequently, the bright-field and fluorescence microscopy images were overlaid in ImageJ, and the insertion depth was expressed as the measured length between the tip of the microneedle and the part up to where the fluorescence was visible.

2.4 Microinjection into skin

To visualize the intradermal injections, a 10 µg/mL fluorescein solution in PBS was injected into human *ex vivo* skin at different depths (100-400 µm). The skin was stretched on Styrofoam covered with parafilm, and the injection depth was adjusted as described above. The microneedle was connected to a syringe pump with a flow rate of 2 µL/min to deliver 3 µL of the fluorescein solution. As a negative control 3 µL of the fluorescein solution was dispensed on top of the skin. Furthermore, diffusion of the injected compound into surrounding tissue was assessed by imaging the fluorescence in the skin at several time points after injection. The fluorescence was imaged using a Microsoft Lifecam HD with a 480±5 nm light source

(LED, Conrad) and a 520-540 nm band pass interference filter.

To confirm that microneedle insertion leads to dermal delivery of the injectable, microinjections of 0.4% trypan blue (Sigma) into *ex vivo* skin were performed at a protrusion depth of 300 µm. Microneedles were inserted into either human or rat skin and subsequently a microinjection of respectively 0.5 µL or 3 µL was performed. Next, 10 µm thick cryosections (Leica Cryostat) of the injected human skin and 5 µm thick cryosections of rat skin were made. Subsequently, the cryosections were stained by hematoxylin and eosin (H&E). Finally, the skin was photographed under a stereo microscope (Zeiss Stemi 2000-c) at a magnification of 5x.

2.5 Immunization

To examine the applicability of the hollow microneedles for vaccination purposes, a comparison was made between vaccination of rats by intradermal injection with microneedles, and intradermal and intramuscular injection with a conventional needle.

Female Wistar Han rats (175-250 g) were obtained from Charles River (Maastricht, the Netherlands) and were maintained under standardized conditions in the animal facility of the Leiden Academic Centre for Drug Research, Leiden University. The study was carried out under the guidelines complied by the animal ethic committee of the Netherlands and was approved by the "Dierexperimentencommisie Universiteit Leiden (UDEC)" under number 12084. Rats (10 per group) were immunized with either 5 or 15 DU ($1/8^{th}$ and $3/8^{th}$ human dose, respectively) IPV-type-1 (1 DU≈13 ng virus protein) [17] intradermally by hollow microneedles at an protrusion depth of 300 µm and a flow speed of 2 µL/min for 4.5 minutes. For comparison, rats were immunized with 5 DU IPV/50 µL intradermally on the ventral abdominal skin with a 30G needle and with 5 DU IPV/200 µL intramuscularly with a 26G needle (100 µL/hind leg). As a negative control rats were injected intramuscularly with 200 µL PBS (100 µL/leg). All rats were anesthetized during the immunization with 50 mg/kg ketamine (Nimatek® (100 mg/mL ketamine, Eurovet Animal Health B.V., Bladel, the Netherlands)) and 5 mg/kg xylazine (Rompun® (20 mg/mL xylazine, Bayer B.V., Mijdrecht, the Netherlands)) by intraperitoneal injection. Three weeks after immunization blood samples were collected and the rats were sacrificed. This immunization scheme is identical to the regular IPV potency assay [18].

2.6 IgG ELISA

Polystyrene 96 wells microtiter plates (Greiner Bio-One, Alphen a/d Rijn, the Netherlands) were coated overnight at 4°C with bovine anti-poliovirus type 1 serum (RIVM, Bilthoven, The Netherlands) in PBS pH 7.2 (Gibco from Invitrogen, Paisley, UK). After washing with 0.05% Tween 80 (Merck, Darmstadt, Germany) in tap water, 100 µL/well monovalent IPV vaccine type 1 (4.5 DU/well) diluted in assay buffer, PBS containing 0.5% (w/v) Protifar (Nutricia, Zoetermeer, the Netherlands) and 0.05% (v/v) Tween 80 (Merck, Darmstadt, Germany), was added. After incubation at 37°C for 2 hours, threefold dilutions of sera samples in assay buffer were added

(100 µL/well) and incubated at 37°C for 2 hours. After washing, plates were subsequently incubated at 37°C for 1 hour with horseradish peroxidase (HRP)-conjugated goat-anti-rat IgG (Southern Biotech, Birmingham, AL) as detection antibody (4000 fold dilution, 100 µL/well). Plates were extensively washed and 100 µl/well TMB substrate solution, containing 1.1 M sodium acetate (NVI, Bilthoven, the Netherlands), 100 mg/mL 3,3',5,5'-tetramethylbenzidine (Sigma-Aldrich, St. Louis, MO), and 0.006% (v/v) hydrogen peroxide (Merck, Darmstadt, Germany), was added. After 10-15 minutes, the reaction was stopped with 100 µL/well 2 M H_2SO_4 (NVI, Bilthoven, the Netherlands) and absorbance was measured at 450 nm by using a Biotek L808 plate reader.

Endpoint titers were determined by 4-parameter analysis using the Gen5™ 2.0 data analysis software (BioTek Instruments, Inc., Winooski, VT) and defined as the reciprocal of the serum dilution producing a signal identical to that of antibody-negative serum samples at the same dilution plus three times the standard deviation [17, 19].

2.7 Virus neutralizing antibodies

Virus neutralizing (VN) antibodies against poliovirus type 1 were measured as described elsewhere [19]. In brief, the sera were inactivated at 56°C for 30 min prior to testing, of which 2 fold serial dilutions were made (2^1 to 2^{24}). These dilutions were incubated with 100 cell culture infectious dose 50% (CCID50) of wild type poliovirus type 1 (Mahoney) for 3 hours at 36°C and 5% CO_2, and the resulting mixtures were subsequently used to inoculate $1{\cdot}10^4$ Vero cells. Virus-neutralizing antibody titers were determined after 7 days by staining the cells with crystal violet and expressed as the last serial dilution with an intact monolayer.

2.8 Statistical analysis

The statistical analysis was performed using Prism 5 for Windows, where the mean ± SEM (n=10) of the IgG and VN titers were calculated. As our data was not-normally distributed, Kruskall-Wallis tests with a Dunns post-hoc test were performed to calculate the statistical significance.

3. Results and discussion

3.1 Production of microneedles: Influence of etch time

The microneedle geometry was observed to be dependent on etch time. The representative different tip shapes that were obtained after 1, 2, 4, 9, 22 and 29 hours of etching (n=3) are depicted in figure 3. Less than four hours of etching resulted in blunt needles with strong etching of the lumen of the capillary. Etch times between 4 and 22 hours resulted in increasingly long, thin needles of up to 4 cm. Longer etching resulted in fully dissolving extended portions of the capillary, leaving a short microneedle with an irreproducible tip shape.

When using a constant etch time reproducibly shaped microneedles were obtained.

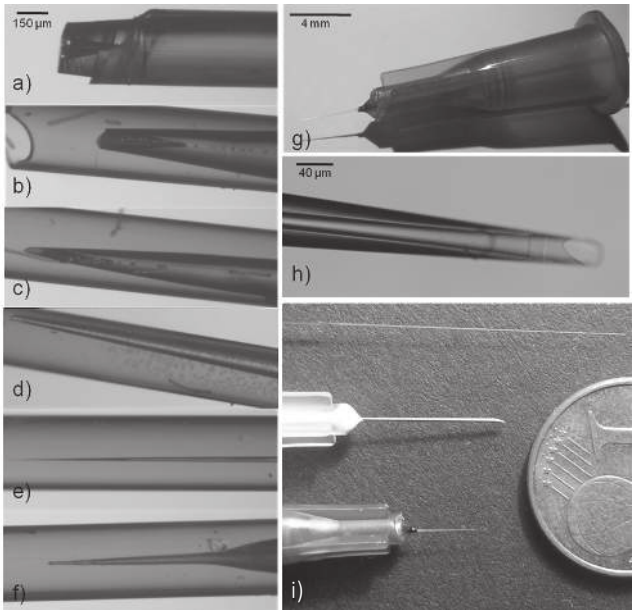

Figure 3: Representative images of the influence of etch time on the tip shape of hollow microneedles etched from capillaries after 1, 2, 4, 9, 22, 29 hours all taken at the same magnification (a-f, respectively); a capillary etched for 4 hours mounted into a Luer hub after removal of the polyimide sleeve, used for dermal drug delivery (g); a typical needle tip opening of microneedles after 4 hours of etching (h); a typical hollow microneedle etched for 22 hours next to a standard 30G needle, a microneedle etched for 4 hours, and a 1 eurocent coin (i).

After 4 hours of etching, microneedles with a tip angle of 15.0°±2.8° were obtained (mean ± SD of 55 microneedles, see supplementary information, figure S1, for angle distribution).

The observed lumen shapes are caused by displacement of the silicone oil. At the start of etching a small amount of HF is sucked into the lumen by capillary force, etching a short length from the inside. After 4 hours this portion is fully etched away, leaving only the part of the capillary that was protected from inside etching (figure 3c, h).

The outer shape of the needle can be explained by the interaction between the HF and the polyimide coating. The coating is slightly permeable to HF. When HF permeates through the coating it slowly etches the fused silica and delaminates the coating and the fused silica. When the coating is separated from the capillary, HF is sucked in between by capillary force. This HF results in the strong etching that determines the final tip shape. As HF supply through the coating is small, mass transport by diffusion from the tip is limiting the etch rate, resulting in slower etching further away from the tip. This gradient in etch rate results in the sharp tip of the microneedle.

Gluing the microneedles into Luer adapters resulted in needles that can be used and connected with the ease of conventional needles (figure 3g).

The relatively short needles obtained by 4 hours of etching were most suitable for injection into the skin because of their rigidity and robustness. While not suitable for injections into the skin, the extremely long needles can be useful for other applications. The ultra-high aspect ratio of these needles (4 cm long, 20 µm tip diameter, figure 3i) could be very useful for deep penetration into soft fragile tissue, e.g., for intracerebral injections.

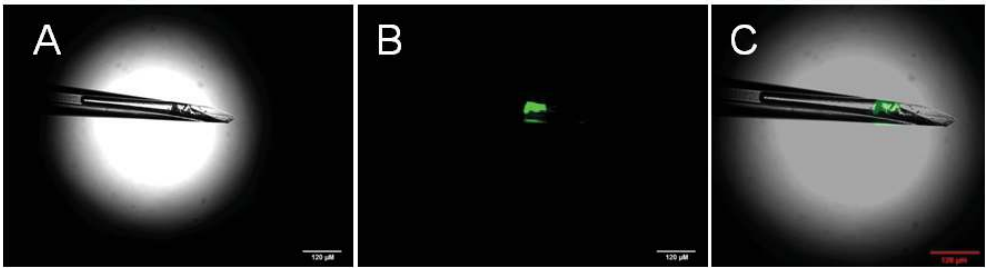

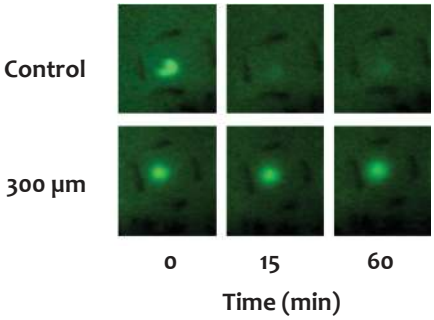

Figure 5: Fluorescence visualization of fluorescein microinjections into *ex vivo* human skin. Control injections (fluorescein dispensed on top of the skin) result in solvent evaporation over time and, consequently, loss of fluorescence, while 300 µm deep injections show no leakage and loss off fluorescence, but prolonged fluorescence inside the skin.

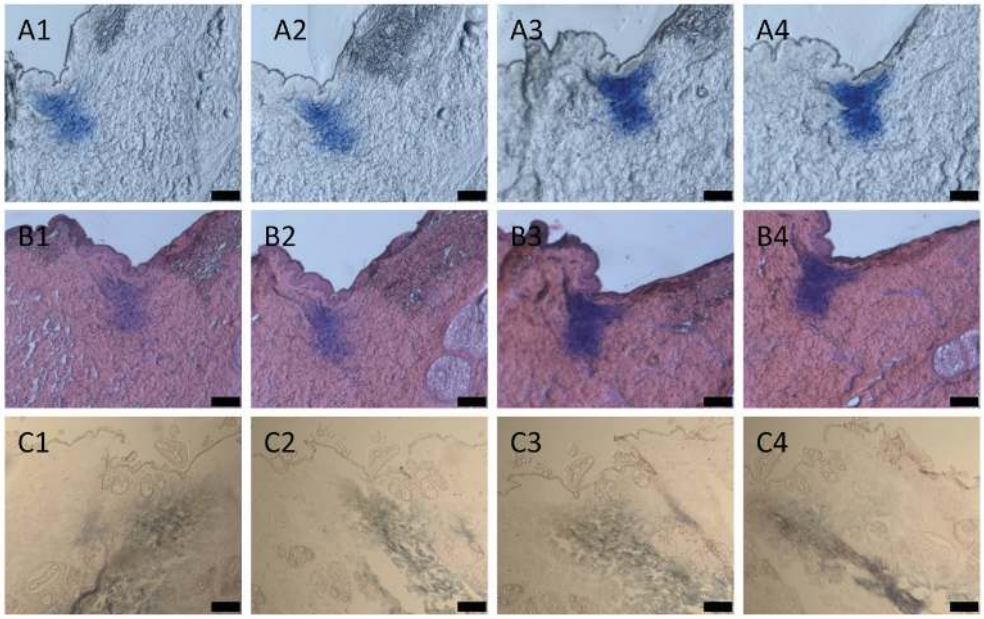

Figure 6: Representative microinjections of trypan blue solution into *ex vivo* skin. Four subsequent 10 µm thick cryosections following a 0.5 µL microinjection into *ex vivo* human skin before (A) and after hematoxylin and eosin (H&E) staining (B). Four subsequent 5 µm thick H&E stained cryosections following a 3 µL microinjection into *ex vivo* rat skin (C). The scale bar is 0.2 mm.

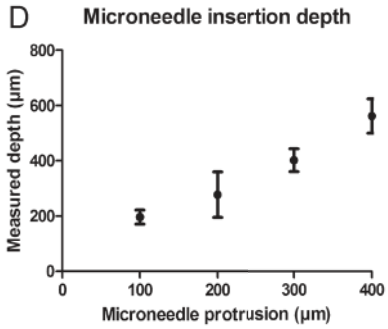

Figure 4: Determination of the depth of microneedle insertion. After hollow microneedles were pierced into fluorescein labeled human skin, one picture of the hollow microneedle was taken by using bright-field microscopy (A), and another picture on the same position was taken by fluorescence microscopy (B). Subsequently, the bright-field and fluorescence microscopy pictures were overlaid (C) from which the depth of microneedle insertion was measured and plotted against the length of the microneedle protruding below the guide-plate (D). Each point in panel D represents the average (± SD) of three individual microneedle insertions.

3.2 Applicator

Microneedle applicators are needed for controlled and reproducible microneedle application and reduce the required insertion forces to pierce the stratum corneum for both solid and hollow microneedles [1, 2, 16, 20-24]. The microneedle applicator used in this work was designed for *in-* and *ex vivo* microinjections with easily adjustable insertion speed, depth, angle, and flow rate. Robust performance was observed, i.e., at an insertion speed of 1 m/s no damage of the needles was observed.

In order to construct the system to be completely air free, gas tight syringes and Luer lock connections combined with pressure resistant fused silica tubing were used. This enables constant flow generation at high pressures. As such, the system could be used at relatively high flow rates without using hyaluronidase (2 µL/min, as compared to literature values of single microneedle injections of 50-300 nL/min) [21, 25, 26]. Flow rates of other systems described in the literature might have been limited by the maximum applicable pressure in systems using common flexible tubing and different pump types [12, 15, 21, 25, 27, 28].

The full tunability of the device is very valuable in a research setting, where varying injections into different skin types and layers are required, e.g., to examine the immune responses as a function of the microneedle insertion depth or injection volume. Whilst completely compatible with use for intradermal microinjections in *in vivo* arms of humans, the freestanding setup of the device is particularly suitable for use in animal studies, as it allows for easy handling of the animals. When used for vaccination of humans, a much simpler applicator with a fixed insertion speed and angle could easily be envisioned. Using a spring loaded, fixed angle applicator would result in a hand held device suitable for a clinical setting.

3.3 Determination of microneedle insertion depth

It is important to control the depth of hollow microneedle insertion into the skin, since this defines whether or not the microneedle injection causes pain and/or bleedings. Fig. 4a-c depicts micrographs of microneedles after insertion into fluorescently labeled *ex vivo* human skin with a velocity of 1 m/s. The distance between the fluorescent dye transferred from the skin and the tip of the needle was used to measure penetration depth. Figure 4d shows that the measured microneedle insertion depth was on average 110±36 µm (mean ± SD,

n=4) deeper than the length of the microneedle protruding past the guide-plate. This offset towards a deeper microneedle insertion than the aimed depth could be due to the pressure that is applied by the microneedle applicator guide-plate onto the skin, causing the skin to bulge into the opening in the plateau (figure 2G). However, when corrected for this offset, this applicator for hollow microneedles enables us to accurately and reproducibly insert a microneedle into the skin at a predetermined depth. A linear correlation (R^2=0.979) between the protrusion length and insertion depth was observed with an average RSD of 16%. The shown depth accuracy is sufficient to selectively inject into the dermis in rats and would allow for even more control in the relatively thick human skin. In addition to the presented results, strain measurements during insertion could be considered for subsequent research to judge the penetration into the different layers of the skin.

3.4 Microinjection into skin

Intradermal injections were visualized by injection of 3 µL fluorescein at a flow speed of 2 µL/min into *ex vivo* human skin. Successful injections were observed at all the injection depths that were tested (100-400 µm). As depicted in figure 5, fluorescence from the injected fluorescein was observed below the surface of the skin. No leakage was observed and fluorescence was maintained for prolonged periods of time. The negative control of fluorescein dispensed on top of the skin showed fast evaporation of the solvent, causing rapid loss of fluorescence intensity. No significant difference in fluorescence intensity between penetration depths from 100-400 µm was observed in the skin (data not shown). Furthermore, no clogging of the microneedles was observed even when the microneedles were used for multiple injections.

To determine whether microneedle insertion leads to dermal delivery of the injectable, microinjections into *ex vivo* skin were performed and the injected site was visualized as shown in figure 6. After a microneedle was inserted into *ex vivo* human skin at a protrusion depth of 300 µm, a microinjection of 0.5 µL 0.4% trypan blue was performed. Four subsequent 10 µm thick cryosections of the injected skin before (6A) and after (6B) H&E staining show that the microinjections are indeed inside the dermis. Furthermore, a microinjection into *ex vivo* rat skin of 3 µL at a protrusion depth of 300 µm also led to the delivery of the injectable into the dermis (6C). Figure 6C shows that trypan blue diffused deep inside the dermis when a volume as large as 3 µL was injected.

3.5 Immunization study

In order to test the applicability of the hollow microneedles for dermal vaccination, rats were immunized with IPV serotype 1. The resulting antibody titers are shown in figure 7. This figure shows that the serum IgG responses after the (intradermal) microinjections with hollow microneedles at a protrusion depth of 300 µm are comparable with those after conventional intramuscular immunization and intradermal immunization, and were comparable to IgG responses found in the literature after a single intramuscular immunization with 5 DU IPV

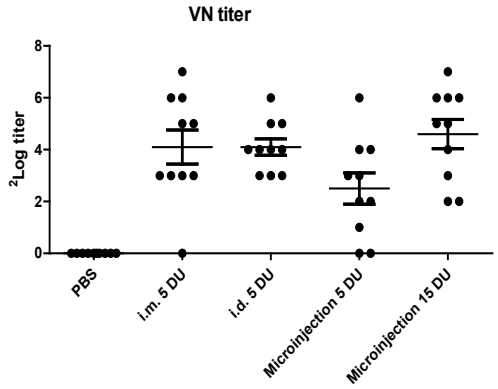

Figure 8: Serum polio-virus neutralizing (VN) antibodies responses after immunization with PBS or 5 DU inactivated poliovirus serotype 1 intramuscularly (i.m.), intradermally (i.d.), or intradermally *via* hollow microneedles with a microinjection of 9 µL containing either 5 or 15 DU IPV.

type 1 [17]. Furthermore, a higher dose IPV (15 DU) delivered by a microinjection of 9 µL appeared to slightly increase the IgG response as compared to a 5 DU microinjection, but the differenece was not statistically significant. Furthermore, no significant differences were observed between the IgG titers of the microneedle injection groups and the intramuscular and intradermal groups.

Besides the serum IgG responses, the rat sera were analyzed for VN antibodies, as shown in figure 8. Despite the slightly lower VN titers of rats intradermally immunized with a microinjection of 5 DU, compared to conventional intramuscular or intradermal immunization, this difference was not significant. The lower VN titer of the microinjection might be caused by reduced damage of the skin compared to intradermal injection, where the needle is much thicker, is injected at a greater depth, and a larger volume is injected. This intrinsic effect of less invasive injections might be overcome by adding an adjuvant to the IPV suspension [1, 19]. Furthermore, the immune responses by intradermal injection might be higher than by intramuscular injection after booster immunizations, since intradermal immunization can lead to accelerated booster responses [11]. Therefore, in future experiments the insertion depth (50-1000 µm), the volume effect (3-50 µL), and the booster effect (up to 3 immunizations) should be evaluated. However, a higher dose of IPV by microinjections led to VN titers comparable to intradermal and intramuscular immunization. Therefore, these data show the applicability of microneedles to successfully induce VN antibodies against polio-virus.

4. Conclusion

Microneedles were fabricated by using a novel cheap and scalable wet etching method that can be employed in a laboratory setting or modified for commercial fabrication. The microneedles were used with a custom-made microneedle applicator for successful depth-controlled intradermal microinjections into human and rat skin. Intradermal microinjection of IPV in rats showed comparable IgG responses to conventional intramuscular injections or intradermal injections. Furthermore, immunization with IPV by microinjection led to the

induction of VN antibodies. Therefore, etched hollow microneedles can offer potentially pain free, minimally-invasive intradermal injections for vaccine delivery. Finally, this hollow microneedle technology enables fundamental research on factors, such as insertion depth, angle of insertion, and volume, on the immune responses after dermal immunization.

Acknowledgements

We thank the Electronics Department at Leiden University for their help in the development of the microneedle applicator. Furthermore, we thank Aat Mulder for preparing the cryosections of rat skin and Pim Schipper for performing the microinjections into *ex vivo* human skin and the subsequent cryosections. This work was (co)financed by the Netherlands Metabolomics Centre (NMC), which is a part of The Netherlands Genomics Initiative/Netherlands Organization for Scientific Research.

References

[1] S.M. Bal, Z. Ding, E. van Riet, W. Jiskoot, J. Bouwstra, Advances in transcutaneous vaccine delivery: do all ways lead to Rome? Journal of Controlled Release 148(3) (2010) 266-282.
[2] K. van der Maaden, W. Jiskoot, J. Bouwstra, Microneedle technologies for (trans)dermal drug and vaccine delivery. Journal of controlled release 161(2) (2012) 645–655.
[3] M.R. Prausnitz, H.S. Gill, J.-H. Park, Modified Release Drug Delivery, Vol. 2nd ed New York: Healthcare, 2008, pp. 295-309.
[4] M.R. Prausnitz, Microneedles for transdermal drug delivery. Adv Drug Deliv Rev 56(5) (2004) 581-587.
[5] O.M. Kew, R.W. Sutter, E.M. de Gourville, W.R. Dowdle, M.A. Pallansch, Vaccine-derived poliovirusus and the endgame strategy for global polio eradication. Annual Review of Microbiology 59(1) (2005) 587-635.
[6] J. E.Salk, UlrichKrech, J. S.Youngner, B. L.Bennett, L. J.Lewis, P. L.Bazeley, Formaldehyde Treatment and Safety Testing of Experimental Poliomyelitis Vaccines. (2011).
[7] P.E.M. Fine, I.A.M. Carneiro, Transmissibility and Persistence of Oral Polio Vaccine Viruses: Implications for the Global Poliomyelitis Eradication Initiative. American Journal of Epidemiology 150 (1999) 1001-1021.
[8] J.F. Modlin, Poliomyelitis in the United States: the final chapter? JAMA: the journal of the American Medical Association 292 (2004) 1749-1751.
[9] N. Nathanson, O.M. Kew, From emergence to eradication: the epidemiology of poliomyelitis deconstructed. American journal of epidemiology 172 (2010) 1213-1229.
[10] K.S. Nelson, J.M. Janssen, S.B. Troy, Y. Maldonado, Intradermal fractional dose inactivated polio vaccine: A review of the literature. Vaccine 30 (2012) 121-125.
[11] J.-F. Nicolas, B. Guy, Intradermal, epidermal and transcutaneous vaccination: from immunology to clinical practice. Expert Review Vaccines 7 (2008) 1201-1214.
[12] S. Chandrasekaran, A.B. Frazier, Mechanical characterization of surface micromachined hollow metallic microneedles. IEEE The Sixteenth Annual International Conference on Micro Electro Mechanical Systems, 2003. MEMS-03 Kyoto (2002) 363 - 366.
[13] S.P. Davis, W. Martanto, M.G. Allen, M.R. Prausnitz, Hollow metal microneedles for insulin delivery to diabetic rats. IEEE Trans. Biomed. Eng 52 (2005) 909-915.
[14] H.J.G.E. Gardeniers, R. Luttge, E.J.W. Berenschot, M.J. de Boer, S.Y. Yeshurun, M. Hefetz, R. van't Oever, A. van den Berg, Silicon micromachined hollow microneedles for Transdermal Liquid Transport. Journal of Microelectromechanical Systems 12 (2003) 855-862.
[15] D.V. McAllister, P.M. Wang, S.P. Davis, J.-H. Park, P.J. Canatella, M.G. Allen, M.R. Prausnitz, Microfabricated needles for transdermal delivery of macromolecules and nanoparticles: Fabrication methods and transport studies. Proc Natl Acad Sci U S A 100 (2003) 13755-13760.
[16] F.J. Verbaan, S.M. Bal, D.J. van den Berg, J.A. Dijksman, M. van Hecke, H. Verpoorten, A. van den Berg, R. Luttge, J.A. Bouwstra, Improved piercing of microneedle arrays in dermatomed human skin by an impact insertion method. Journal of Controlled Release 128 (2008) 80-88.
[17] J. Westdijk, D. Brugmans, J. Martin, A. van't. Oever, W.A.M. Bakker, L. Levels, G. Kersten, Characterization and standardization of Sabin based inactivated polio vaccine: Proposal for a new antigen unit for inactivated polio vaccines. Vaccine 29 (2011) 3390-3397.

[18] G. van Steenis, A. van Wezel, V. Sekhuis, Potency testing of killed polio vaccine in rats. Developments in biological standardization 47 (1981) 119-128.
[19] J. Westdijk, P. Koedam, M. Barro, B.P. Steil, N. Collin, T.S. Vedvick, W.A.M. Bakker, P. van der Ley, G. Kersten, Antigen sparing with adjuvanted inactivated polio vaccine based on Sabin strains. Vaccine 31 (2013) 1298-1304.
[20] M. Cormier, B. Johnson, M. Ameri, K. Nyam, L. Libiran, D.D. Zhang, P. Daddona, Transdermal delivery of desmopressin using a coated microneedle array patch system. Journal of Controlled Release 97 (2004) 503-511.
[21] P.M. Wang, M. Cornwell, J. Hill, M.R. Prausnitz, Precise microinjection into skin using hollow microneedles. Journal of Investigative Dermatology 126 (2006) 1080-1087.
[22] M.I. Haq, E. Smith, D.N. John, M. Kalavala, C. Edwards, A. Anstey, A. Morrissey, J.C. Birchall, Clinical administration of microneedles: skin puncture, pain and sensation. Biomed Microdevices 11 (2009) 35-47.
[23] M. Yang, J.D. Zahn, Microneedle insertion force reduction using vibratory actuation. Biomed Microdevices 6 (2004) 177-182.
[24] M.L. Crichton, A. Ansaldo, X. Chen, T.W. Prow, G.J.P. Fernando, M.A.F. Kendall, The effect of strain rate on the precision of penetration of short densely-packed microprojection array patches coated with vaccine. Biomaterials 31 (2010) 4562-4572.
[25] W. Martanto, J.S. Moore, O. Kashlan, R. Kamath, P.M. Wang, J.M. O'Neal, M.R. Prausnitz, Microinfusion using hollow microneedles. Pharmaceutical Research 23 (2006) 104-113.
[26] N. Roxhed, B. Samel, L. Nordquist, P. Griss, G. Stemme, Painless drug delivery through microneedle-based transdermal patches featuring active infusion. IEEE transactions on bio-medical engineering 55 (2008) 1063 - 1071.
[27] S.-J. Paik, S. Byun, J.-M. Lim, Y. Park, A. Lee, S. Chung, J. Chang, K. Chun, D.D. Cho, In-plane single-crystal-silicon microneedles for minimally-invasive microfluid systems. Sensors and Actuators A: Physical 2004 (2004) 276–284.
[28] Q. Cui, C. Liu, X.F. Zha, Study on a piezoelectric micropump for the controlled drug delivery system Microfluid Nanofluid 3 (2007) 377–390.

Supplementary information

To assess the variation in the dimensions of the tip angle, a batch of 55 microneedles etched from 20 µm ID capillaries, etched for four hours, was measured as shown in figure S1. The batch of 55 needles had an average tip angle of 15.0° ± 2.8° (mean ± SD).

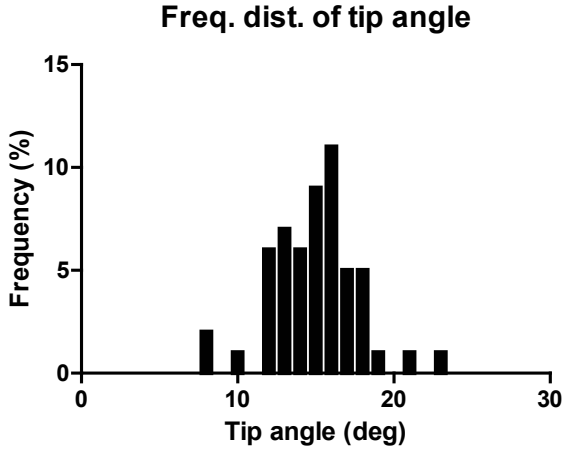

Figure S1: Distribution of the tip angle of 55 microneedles etched for four hours from 20 µm ID capillaries.